Membrane Potentials across Cation-Exchange Membranes with a Low Water Content

Ryotaro Yamamoto, Hidetoshi Matsumoto, and Akihiko Tanioka*

Department of Organic and Polymeric Materials, and International Research Center of Macromolecular Science, Tokyo Institute of Technology, 2-12-1 Ookayama, Meguro-ku, Tokyo 152-8552, Japan

Received: January 28, 2003; In Final Form: June 22, 2003

A study of the effective charge density of a charged membrane with a low water content was carried out. The membrane potentials across charged membranes, which have various water contents and an inhomogeneous fixed charge distribution, were measured. The experimental results were analyzed on the basis of the Donnan equilibrium theory and the Nernst−Planck transport equation considering the fixed charge inhomogeneities in the membrane. The results show that the value of the charge effectiveness will depend on the membrane water content, the ionic radii of the counterions, and the valence of the counterion. To interpret the variation in the value of the charge effectiveness, we attempted to introduce the concept of an ion pair between the fixed charge group and counterion inside the membrane. Compared with the experimental results, the prediction of the ion pair theory qualitatively agreed with the experimental tendency. This suggests that ion pairs cause the difference between the effective charge density and the fixed charge density, especially for a low water content condition.

Introduction

The fixed charge density of the charged membrane estimated by the ionic transport procedure is less than that by the equilibrium procedure.[1−3] It has been considered that this phenomenon is a result of the membrane inhomogeneities or ion pairs between the fixed charge group and counterion in the membrane.[4−16] The membrane has structural inhomogeneities on a macroscopic or microscopic scale generated by the membrane fabrication process. The transport properties (permselectivity and current−voltage characteristics) are strongly affected by the existence of these inhomogeneities; Reiss et al. have shown that an inhomogeneous distribution of fixed charge groups gives rise to increase current efficiency.[6,7] Petropoulos has pointed out that the theory based on structural inhomogeneities of the membranes with a relatively high water content appears to be appropriate to explain the difference in the effective charge density obtained by the transport procedure from the net charge density.[9] While the ionic transport phenomena across charged membranes are strongly affected by the fixed charge groups, since the region in the charged membrane, especially for the low water content condition or in an organic solvent is a relatively low dielectric constant. In accordance with the ion pair theory, most of the fixed charge groups in the membranes are neutralized by the counterions due to the formation of the ion pairs.[13] Therefore, the effective charge density is decreased. Chou et al. showed that by considering the ion pairs between the fixed charge group and counterion, the theoretical predictions of the membrane potentials and permeability coefficients across the membrane in the organic solvent are in good agreement with the experimental results.[14−16]

On the other hand, the studies and experimental data for the membranes with low water contents are limited. In this study, the membrane potentials across the charged membranes, which have various water contents, are measured in order to understand ionic transport phenomena across the charged membranes under such conditions. In addition, to obtain information about the fixed charge inhomogeneities of the membrane, an analysis of the fixed charge distribution across the thickness of the membrane is performed using energy dispersive X-ray analysis (EDX). EDX line scan on the cross section of charged membranes showed that most of the fixed charge groups exist near the membrane surface region. According to the studies of Teorell, Meyer, and Sievers (TMS),[17−19] the membrane potentials in a charged membrane can theoretically be expressed by the Donnan equilibrium theory[20,21] and the Nernst−Planck transport equation,[22] if it is assumed that the fixed charge groups are homogeneously distributed in the membrane. In contrast, in the case of inhomogeneous membranes, an additional assumption must be required, for example, a constant ion concentration gradient[23] or a constant electric potential gradient[24] in a membrane. Recently, Mafé et al. developed a theory to analyze the transport properties across membranes with an inhomogeneous fixed charge distribution.[11] Using this theory, we can calculate the potential difference across not only a homogeneous membrane, but also across the inhomogeneous membrane without these assumptions. The calculation results are compared with the experimental ones, and we discuss the effects of the ion pairs between the fixed charge group and counterion on the effective charge density of the membrane with a low water content.

Theory

The membrane transport system in this study is shown in Figure 1. The charged membrane, whose thickness is d, separates two solutions of the same electrolyte. $C_i(x)$ represents the concentration of the ith species at a point of coordinate x within the membrane ($i = 1$ for salt cation, $i = 2$ for salt anion, and $i = X$ for fixed charge group). $C_{i\mathrm{L}}$ and $C_{i\mathrm{R}}$ denote the concentration of the ith species in the bulk electrolyte solutions for the left-side cell and the right-side cell, respectively.

* Author to whom correspondence should be addressed. Tel: +81-3-5734-2426. Fax: +81-3-5734-2876. E-mail: atanioka@o.cc.titech.ac.jp.

10.1021/jp0342273 CCC: $25.00
Published on Web 08/27/2003

The basic equation describing the ionic transport through the charged membrane is the Nernst−Planck equation.

$$J_i = -D_i\left(\frac{dC_i}{dx} + z_i C_i \frac{F}{RT}\frac{d\phi}{dx}\right) \quad (1)$$

where J_i and D_i are the ionic flux and the diffusion coefficient of the ith species in the membrane and ϕ is the local electric potential in the membrane. In this system, the electric current density should be equal to zero:

$$z_1 J_1 + z_2 J_2 = 0 \quad (2)$$

The condition of electroneutrality in the membrane and in the bulk electrolyte solutions requires that

$$z_1 C_1 + z_2 C_2 + z_x C_x = 0 \quad (3)$$

$$z_1 C_{1j} = -z_2 C_{2j} = -z_1 z_2 C_{sj} \quad j = \mathrm{L,R} \quad (4)$$

where C_{sj} is the salt concentration in the bulk electrolyte solutions.

According to the Donnan equilibrium, both the ionic concentration and electric potential are assumed to be discontinuous at the membrane−solution interfaces. The concentrations of the cation and anion then obey the following equations:

$$C_1(0)^{-z_2}\left\{C_1(0) + \frac{z_x}{z_1}C_x(0)\right\}^{z_1} - \left(\frac{\gamma_1}{k_1\gamma_{1\mathrm{L}}}\right)^{z_2}\left(\frac{\gamma_2}{k_2\gamma_{2\mathrm{L}}}\right)^{-z_1}(z_2 C_{s\mathrm{L}})^{z_1-z_2} = 0 \quad (5)$$

$$C_2(0)^{z_1}\left\{C_2(0) + \frac{z_x}{z_2}C_x(0)\right\}^{-z_2} - \left(\frac{\gamma_1}{k_1\gamma_{1\mathrm{L}}}\right)^{z_2}\left(\frac{\gamma_2}{k_2\gamma_{2\mathrm{L}}}\right)^{-z_1}(-z_1 C_{s\mathrm{L}})^{z_1-z_2} = 0 \quad (6)$$

$$C_1(d)^{-z_2}\left\{C_1(d) + \frac{z_x}{z_1}C_x(d)\right\}^{z_1} - \left(\frac{\gamma_1}{k_1\gamma_{1\mathrm{R}}}\right)^{z_2}\left(\frac{\gamma_2}{k_2\gamma_{2\mathrm{R}}}\right)^{-z_1}(z_2 C_{s\mathrm{R}})^{z_1-z_2} = 0 \quad (7)$$

$$C_2(d)^{z_1}\left\{C_2(d) + \frac{z_x}{z_2}C_x(d)\right\}^{-z_2} - \left(\frac{\gamma_1}{k_1\gamma_{1\mathrm{R}}}\right)^{z_2}\left(\frac{\gamma_2}{k_2\gamma_{2\mathrm{R}}}\right)^{-z_1}(-z_1 C_{s\mathrm{R}})^{z_1-z_2} = 0 \quad (8)$$

We then define the value Q as follows:

$$Q = \left(\frac{\gamma_1}{k_1\gamma_{1j}}\right)^{z_2/(z_2-z_1)}\left(\frac{\gamma_2}{k_2\gamma_{2j}}\right)^{-z_1/(z_2-z_1)} \quad j = \mathrm{L,R} \quad (9)$$

where Q is a constant which indicates the effectiveness of the fixed charge.

While the electric potentials at the left ($\Delta\phi_\mathrm{L}$) and right ($\Delta\phi_\mathrm{R}$) interfaces are given as follows:

$$\Delta\phi_\mathrm{L} = -\frac{RT}{z_i F}\ln\frac{\gamma_i C_i(0)}{k_i\gamma_{i\mathrm{L}}C_{i\mathrm{L}}} \quad (10)$$

$$\Delta\phi_\mathrm{R} = \frac{RT}{z_i F}\ln\frac{\gamma_i C_i(d)}{k_i\gamma_{i\mathrm{R}}C_{i\mathrm{R}}} \quad (11)$$

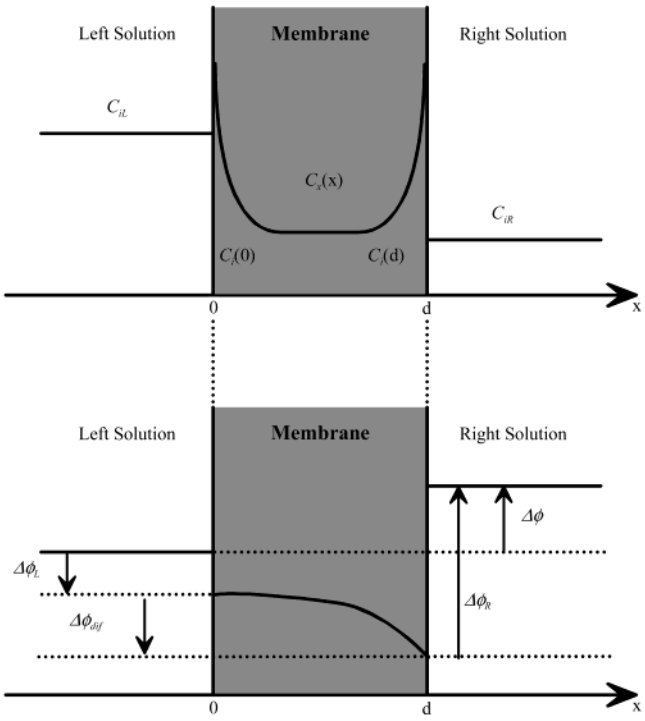

Figure 1. Schematic diagram of the membrane transport system.

where γ_i and γ_{ij} (j = L and R) are the activity coefficients in the membrane and the bulk electrolyte solution, z_i and k_i represent the valence and the partition coefficient of the ith species, respectively, R is the gas constant, T is the absolute temperature, and F is Faraday's constant.

At first, it is assumed that the concentration dependence of the activity coefficients of all ions is negligible. The sum of the Donnan potentials ($\Delta\phi_\mathrm{Don}$) can then be written as

$$\Delta\phi_\mathrm{Don} = \Delta\phi_\mathrm{L} + \Delta\phi_\mathrm{R} = -\frac{RT}{z_i F}\ln\frac{C_{i\mathrm{R}}C_i(0)}{C_{i\mathrm{L}}C_i(d)} \quad (12)$$

By reordering eqs 1 and 3, the following expressions are derived:

$$\frac{d\phi}{dx} = \frac{\left(1 - \frac{z_2}{z_1}\right)\frac{dC_2}{dx} - \frac{z_x}{z_1}\frac{dC_x}{dx} + \frac{J_1}{D_1} + \frac{J_2}{D_2}}{\frac{F}{RT}z_x C_x} \quad (13)$$

$$\frac{dC_2}{dx} = \frac{-\left\{z_2 C_2\left(-\frac{z_x}{z_1}\frac{dC_x}{dx} + \frac{J_1}{D_1} + \frac{J_2}{D_2}\right) + z_x C_x \frac{J_2}{D_2}\right\}}{z_2 C_2\left(1 - \frac{z_2}{z_1}\right) + z_x C_x} \quad (14)$$

To obtain the ionic concentration and the electric potential profile in the membrane, eqs 13 and 14 must be solved using eqs 5−8 as boundary conditions. We have employed the following iterative procedure:

(1) We assume an arbitrary value for the cationic flux J_1.

(2) Equation 14 is solved using the fourth-order Runge−Kutta method with the boundary conditions at the left interface.

(3) We check the boundary conditions at the right interface. The initial value of the cationic flux is changed, and the numerical calculation is repeated until the solution is satisfied by the boundary conditions at the right interface.

TABLE 1: Membrane Preparation Condition

	w_{St}[a]	w_{DVB}[b]	w_{PBO}[c]	$t_{sulfonation}$[d]
CEM04	50	50	1	10
CEM07	90	10	1	10
CEM16	90	10	1	20
CEM27	95	5	1	20

[a] w_{St} [wt %]: weight ratio of styrene in the monomer solutions. [b] w_{DVB} [wt %]: weight ratio of divinylbenzene in the monomer solutions. [c] w_{PBO} [wt %]: weight ratio of Perbutyl O in the monomer solutions. [d] $t_{sulfonation}$ [h]: sulfonation time.

We can then obtain the electric potential profile within the membrane to integrate eq 13. The diffusion potential ($\Delta\phi_{dif}$) in the membrane is calculated as

$$\Delta\phi_{dif} = \phi(d) - \phi(0) \tag{15}$$

According to the studies of Teorell, Meyer, and Sievers (TMS), the potential difference across a membrane, which separates the two solutions of different concentrations, can be expressed by the sum of the Donnan potentials at the left and right interfaces and the diffusion potential in the membrane:

$$\Delta\phi = \Delta\phi_L + \Delta\phi_{dif} + \Delta\phi_R \tag{16}$$

Experimental Section

Materials. The polyethylene (PE) porous membranes (Hipore H-4050U3) were obtained from Asahi Kasei Corporation, Japan. Styrene and 55% divinylbenzene (mixture of isomers) were purchased from Wako Pure Chemical, Japan. *tert*-Butylperoxy-2-ethylhexanoate (Perbutyl O) was purchased from NOF Corporation, Japan.

Preparation of the Base Membranes.[25−29] PE porous membranes were used as the substrate. The rectangular PE samples (40 mm × 40 mm) were washed in methanol for 24 h and dried before use. These membranes were immersed in the monomer solutions, which were composed of styrene, 55% divinylbenzene, and Perbutyl O. The mixing ratio of styrene to 55% divinylbenzene was varied to control the membrane water content. After immersion in the monomer solutions under 10 °C for 16 h, the membranes were sandwiched between two poly(ethylene terephthalate) films. The copolymerization was then done at 70 °C for 32 h. The membranes were removed from the films and left for 1 day at room temperature.

Sulfonation Procedure. The base membranes were immersed in concentrated sulfuric acid at 70 °C. To obtain the membranes with different water contents, the sulfonation time was varied. The detailed reaction conditions are listed in Table 1. After the proper time, the membranes were extracted from the concentrated sulfuric acid, then washed two times in methanol and subsequently in deionized water to remove the excess sulfuric acid in the membranes.

Physicochemical Properties of the Membranes Used in This Study. To obtain the physicochemical properties used in this study, the potentiometric titration measurements and water content measurements were performed.

The potentiometric titration measurements were performed using a combination electrode (GST-5721C, TOA Electronics, Japan) and a pH meter (HM-60G, TOA Electronics, Japan). First, the membranes were immersed in 2 mol/L HCl solution for 24 h to ensure that the counterions were exchanged for H^+. After sufficiently washing the membranes in deionized water, two pieces of the membrane (each membrane area was 16 cm^2) were soaked in 3 mol/L KCl solution under a nitrogen gas flow with stirring for 1 h to elute the H^+ ions from the membranes.

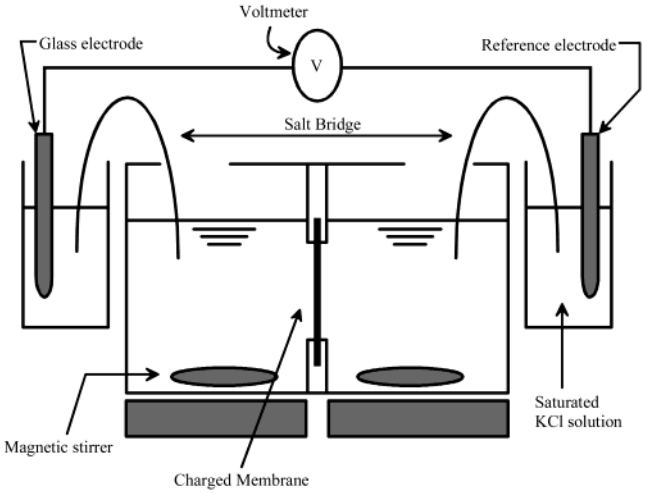

Figure 2. Schematic diagram of the apparatus for the membrane potential measurements.

They were then titrated by adding a 0.1 mol/L KOH solution to obtain the titration curve. The amount of the fixed charge group (N_X) in the membranes is equal to the titer of KOH.

The membranes used in the potentiometric titration measurements were immersed in 3 mol/L NaCl solution for 24 h to exchange the counterions for Na^+. The membranes were then sufficiently washed in deionized water. After removing the membrane surface water, the membrane weight in the equilibrium swollen state (w_{wet}) was measured. Subsequently, the membranes were dried in a vacuum oven at 25 °C for 6 h, and the membrane weight in the dry state (w_{dry}) was determined.

The water content (w_w) of the membranes is defined by the following equation:

$$w_w = \frac{w_{wet} - w_{dry}}{w_{wet}} \tag{17}$$

The ion-exchange capacity (IEC) and the fixed charge density (C_X) are determined by the following equations:

$$\mathrm{IEC} = \frac{N_X}{w_{dry}} \tag{18}$$

$$C_X = \frac{N_X}{w_{wet} - w_{dry}} \tag{19}$$

Distribution of the Fixed Charge Groups across the Membrane. An analysis of the fixed charge distribution across the thickness of the membrane was performed using the energy-dispersive X-ray (EDX) attachment of a Hitachi S-800 field emission gun and a scanning electron microscope (FE-SEM). According to an EDX elemental analysis of S along the direction of the membrane thickness, the distribution of the sulfonic acid groups inside the membrane was monitored.

Measurement of the Membrane Potential. The membrane potentials of the membranes used in this study were measured to obtain information regarding the interaction between the fixed charge groups and counterions in the membrane with a low water content. The apparatus for measurement of the membrane potentials is shown in Figure 3. A charged membrane was placed in the center of two containers. Both containers were filled with electrolyte solutions of different concentrations; the left container was kept constant at 10^{-3} mol/L, while that on the right was

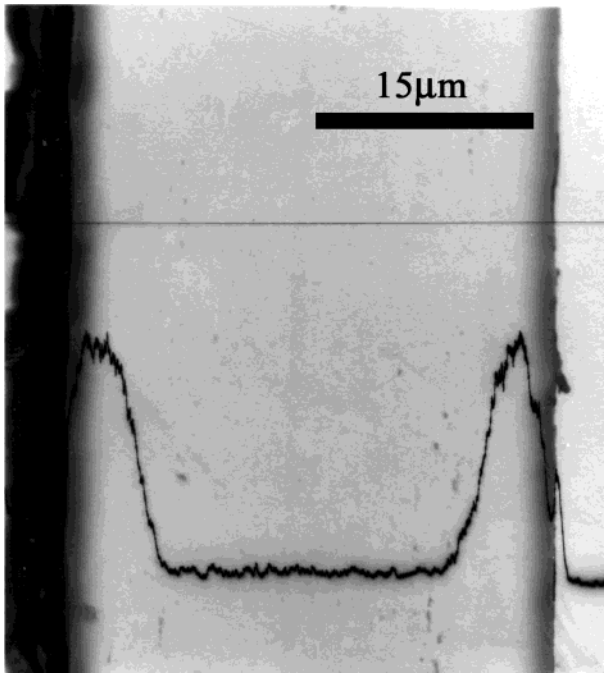

Figure 3. Cross-sectional SEM image of a cation-exchange membrane (CEM04) with the intensity of the S Kα of the EDX line scan.

TABLE 2: Physicochemical Properties of a Membrane Composed of Poly(divinylbenzene-*co*-styrene) Containing Sulfonic Acid Groups

	w_{water}[a]	IEC[b]	C_X[c]	d[d]
CEM04	3.5	0.4	11	50
CEM07	7.2	0.3	4.6	50
CEM16	16	1.2	3.3	50
CEM27	27	1.4	1.9	50
K501	30	1.5	5.5	170

[a] w_{water} [wt %]: water content of the membrane. [b] IEC [meq/g (dry membr.)]: ion-exchange capacity of the membrane. [c] C_X [mol/l]: fixed charge density of the membrane. [d] d [μm]: thickness of the membrane.

varied from 10^{-3} to 3 mol/L. A voltmeter (HM-40S, TOA Electronics, Japan) connected to glass electrodes (HS-205C, TOA Electronics, Japan) was used for measurement of the potential difference. Two glass electrodes were placed in saturated KCl solutions, which were connected to the containers by KCl salt bridges. KCl, NaCl, LiCl, $CaCl_2$, and $MgCl_2$ were used to measure the membrane potentials. The solutions in both containers were stirred by magnetic stirrers to minimize the effect of the boundary layers on the membrane potential.

Results and Discussion

The physicochemical properties of the membranes used in this study are listed in Table 2 together with that of a commercial cation-exchange membrane (Aciplex K501: Asahi Kasei Corporation) for comparison. The various membranes with different water contents can be obtained by changing the mixing ratio of styrene to divinylbenzene and the sulfonation time. The water content of all the membranes is smaller than that of K501.

A cross-sectional SEM image of a cation-exchange membrane (CEM04) with the intensity of the S Kα of the EDX line scan is shown in Figure 4. According to the EDX elemental analysis of S along the direction of the membrane thickness, most of the fixed charge groups exist near the membrane surface region. Hence, CEM04 has a fixed charge density decreasing from the membrane surface to the membrane interior. Similar profiles of the fixed charge groups are obtained for the others. Hence,

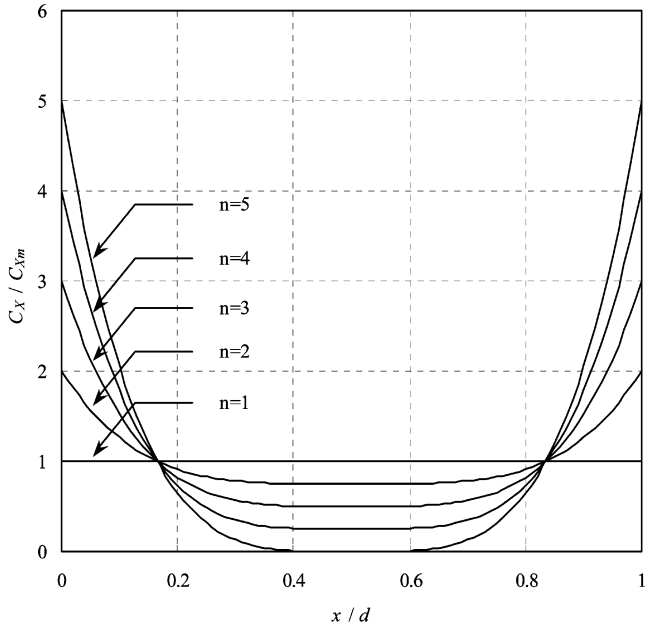

Figure 4. Theoretical model for the distribution of the fixed charge groups across the membrane for different values of n.

we define the dependence of the fixed charge density on the distance from the membrane surface as follows:

$$C_X(x) = C_{X_0}\left(\frac{5-n}{4n} + \frac{5}{4}\frac{n-1}{n}\left(1 - 2\frac{x}{d}\right)^4\right) \quad 1 \le n \le 5 \quad (20)$$

where C_{X_0} is the maximum value of the fixed charge density. Note that parameter n represents the degree of the membrane inhomogeneity. Figure 5 shows that the membrane inhomogeneity increases with n, and if the value n equals unity, the membrane is homogeneous. The average fixed charge density, C_{X_m}, is defined as follows:

$$C_{X_m} = \frac{1}{d}\int_0^d C_X(x)\mathrm{d}x = \frac{C_{X_0}}{n} \quad (21)$$

The average fixed charge density can be experimentally obtained by the potentiometric titration measurements, and thus the maximum value of the fixed charge density can be calculated by solving eq 21.

Figure 5 shows the results of the membrane potentials for CEM04, CEM07, CEM16, and CEM27, respectively. The membrane potentials increase as the salt concentration of the bulk electrolyte solutions (C_{sL}) increase, except for CEM04 measured in the presence of divalent counterions. On the other hand, the membrane potentials of CEM04 in the $CaCl_2$ and $MgCl_2$ solutions go through a maximum as the salt concentration increases.

The membrane potentials are also calculated using eqs 12−16 and are plotted in Figure 5 as a solid line for the membrane model with an inhomogeneous fixed charge distribution ($n > 1$) and as a dotted line for the homogeneous membrane model ($n = 1$). The calculation results using the homogeneous membrane model do not agree with the experimental data, in particular the electrolyte is $CaCl_2$ or $MgCl_2$. In contrast, taking the inhomogeneous fixed charge distribution into account in the membrane potential theory, the theoretical estimations are in good agreement with the experimental results. These results show that it is necessary to consider the membrane inhomogeneity in the membrane potential theory to accurately describe the membrane potential profiles, though the membranes have been treated as homogeneous in the TMS theory, because the

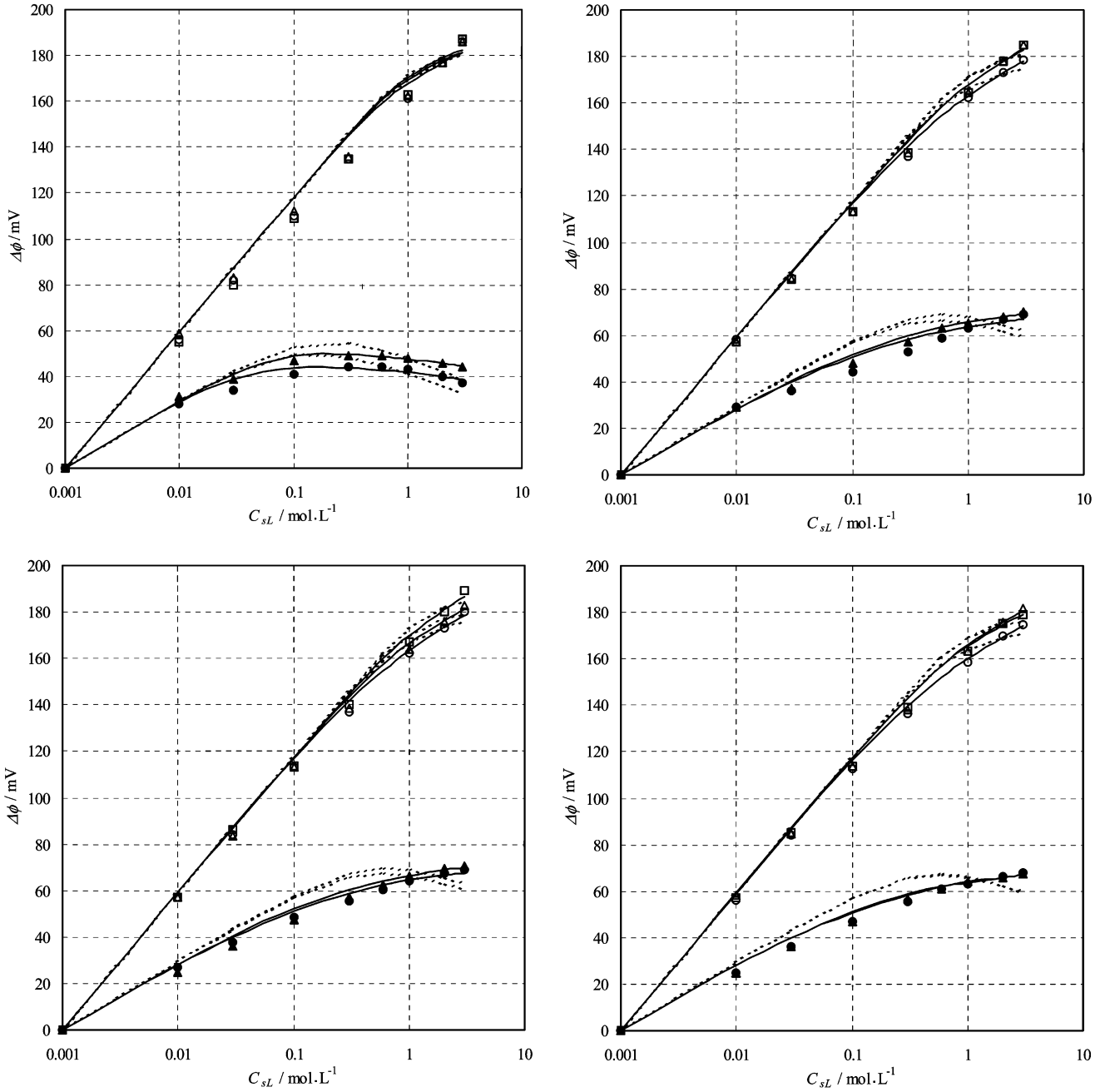

Figure 5. Membrane potentials of cation-exchange membranes for the various electrolytes as a function of the salt concentration in the bulk electrolyte solutions (C_{sL}): For (a) CEM04, (b) CEM07, (c) CEM16, and (d) CEM27. ○, △, □, ●, and ▲ represent the experimental data for KCl, NaCl, LiCl, $CaCl_2$, and $MgCl_2$, respectively. Solid lines indicate the theoretical results obtained by fitting the experimental data to eqs 12−16 considering the inhomogeneous fixed charge distribution in the membrane. Dotted lines are the theoretical results obtained by fitting the experimental data to eqs 12−16 neglecting the inhomogeneous fixed charge distribution in the membrane.

TABLE 3: Values of the Charge Effectiveness (*Q*)

	KCl	NaCl	LiCl	$CaCl_2$	$MgCl_2$
CEM04	0.12	0.18	0.24	0.021	0.038
CEM07	0.21	0.50	0.65	0.31	0.47
CEM16	0.31	0.61	1.1	0.46	0.71
CEM27	0.39	1.0	1.2	0.75	0.93

membrane has structural inhomogeneities on a macroscopic or microscopic scale generated by the membrane fabrication process. The values of the charge effectiveness, *Q*, estimated by fitting the experimental results to the theoretical ones are shown in Table 3. Most of the *Q* values are not equal to unity. This means that we must consider not only the membrane inhomogeneity but also another reason such as the electrostatic interaction between the fixed charge group and counterion to explain the difference in the effective charge density from the fixed charge density. From Table 3, we can then indicate the following three features of the *Q* values. (1) The *Q* value decreased with the membrane water content decrease or the increment of the fixed charge density of the membrane. (2) For the 1−1 type electrolyte system, the order of the *Q* value is LiCl > NaCl > KCl; for the 2−1 type electrolyte system, it is $MgCl_2$ > $CaCl_2$. In other words, the *Q* value decreases with the increasing ionic radii of the counterions, if an ion has the same valence. (3) The *Q* value decreases with the valence of the counterion except for CEM07, CEM16, and CEM27 measured in KCl solution.

On the other hand, in accordance with the ion pair theory, ionic transport phenomena across charged membranes are

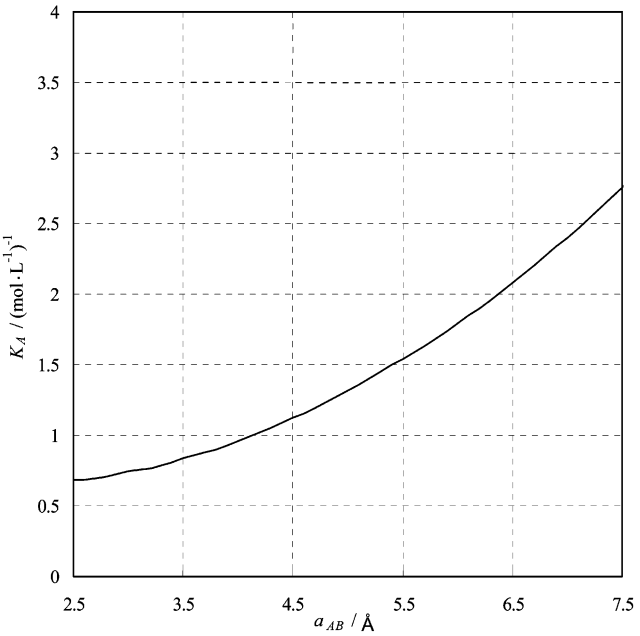

Figure 6. Association constant (K_A) between the counterion and the fixed charge groups in the membrane as a function of the center-to-center distance (a_{AB}) in the 1−1 type electrolyte system calculated by eq 23 for $z_A = 1$, $z_B = -1$, $T = 298.15$ K, and $\epsilon_r = 78$.

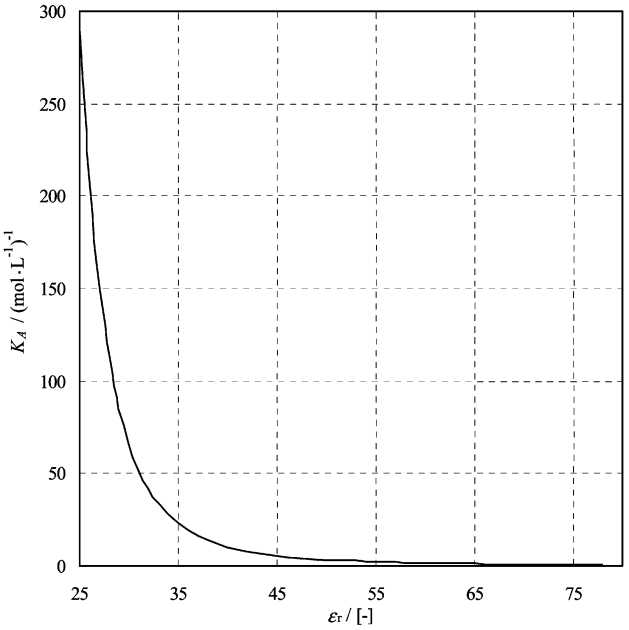

Figure 7. Association constant (K_A) between the counterion and the fixed charge groups in the membrane as a function of the dielectric constant (ϵ_r) in the 1−1 type electrolyte system calculated by eq 23 for $z_A = 1$, $z_B = -1$, $T = 298.15$ K, and $a_{AB} = 2.5$ Å.

strongly affected by the fixed charge groups, since the region in the charged membrane is a relatively low dielectric constant. Thereby most of the fixed charge groups in the membranes are neutralized by the counterions due to the formation of ion pairs. As a result, the effective charge density is decreased. The Q value is related to the association constant (K_A) between the counterion (A) and the fixed charge group (X) in the membrane and expressed by eq 23 as a function of K_A.

$$X + A \overset{K_A}{\rightleftharpoons} XA \tag{22}$$

$$Q \sim \frac{1}{K_A + 1} \tag{23}$$

Application of the Fuoss formalism[30,31] to the ion pair in a membrane would lead to the association constant.

$$K_A = \frac{4\pi N_A}{3 \times 10^{-3}} a_{AB}^3 \exp\left(\frac{z_A z_B q^2}{4\pi\epsilon_\upsilon \epsilon_r a_{AB} k_B T}\right) \tag{24}$$

where N_A is Avogadro's number, q is the electronic charge, ϵ_υ and ϵ_r are the dielectric constant of the vacuum and solvent, respectively, a_{AB} is the center to center distance between ions, and k_B is the Boltzmann constant. From eq 23, the more the fixed charge groups in the membrane pair with the counterions, the more the effective charge density is decreased. Figure 6 shows the K_A dependence on a_{AB} in the 1−1 type electrolyte system. From Figure 6, K_A is increased as the center to center distance a_{AB} increases. For the ion pair in a membrane, the fixed charge groups pair with the counterions. Therefore, the order of the center-to-center distance is determined by the ionic radii of the counterions. The crystallographic radii of the ions are listed in Table 4.[32] The order of the ionic radii is $Li^+ < Na^+ < K^+$ for monovalent ions, and $Mg^{2+} < Ca^{2+}$ for divalent ions; the order of the Q value is $K^+ < Na^+ < Li^+$ for monovalent ions, and $Ca^{2+} < Mg^{2+}$ for divalent ions. The K_A also depends on the valence of the ions (z_A, z_B). K_A calculated for the 1−1, 2−2, and 3−3 type electrolyte systems are given in Table 5. It

TABLE 4: Ionic Radii of Ions

	K^+	Na^+	Li^+	Ca^{2+}	Mg^{2+}
r_{cry}[a]	1.38	1.02	0.74	1.00	0.72

[a] r_{cry} [Å]: crystallographic radius of ion.

TABLE 5: Association Constant (K_A) Calculated for 1−1, 2−2, and 3−3 Type Electrolyte Systems

	1−1	2−2	3−3
K_A	0.973	213	1.69×10^6

shows that K_A for ions with a higher valence is greater than that for ions with a lower valence. Besides, K_A is related to the dielectric constant near the fixed charge groups and plotted as a function of the dielectric constant in Figure 7. K_A increases with the decreasing dielectric constant. In accordance with Booth,[33] the dielectric constant is dependent on the electric field. Hence, in the membrane, the dielectric constant near the pore surface is lower than that of the bulk value due to the electric field generated by the fixed charge and decreased as the surface charge density of the membrane pore surface increases. The surface charge density is related to the fixed charge density; if the membrane has a cylindrical pore with a uniformly distributed fixed charge, the surface charge density of the membrane pore surface is given as follows.[34,35]

$$\sigma = \frac{F r_0 C_X}{2} \tag{25}$$

where σ is the surface charge density and r_0 is the pore radius. Therefore, the surface charge density is in proportion to the fixed charge density of the membrane or is inversely proportional to the membrane water content. As a result, K_A increases with the increment of the fixed charge density of the membrane or the membrane water content decrease.

As these predictions by the ion pair theory compare with the experimental results, feature 1 and feature 2 of the Q value cited above can be qualitatively explained. As for feature 3, the prediction by the ion pair theory is different from the experi-

mental result; from ion pair theory, the *Q* value for divalent ions is smaller than that for monovalent ions. The experimental results, however, show that the *Q* value for KCl is the smallest of all the electrolytes used in this study except for CEM04. This fact can be caused by the effect of hydration on the solute−solute interaction. Desnoyers and co-workers[36] proposed a structural hydration interaction (SHI) model based on that effect to account for the many thermodynamic properties of small solutes in water. Satoh et al.[37] applied the SHI model to the study of the counterion binding of polyelectrolytes in order to explain the experimental fact that the specific counterion binding was not observed in the polysulfate and polysulfonate/Mg^{2+}, Ca^{2+} systems but in the polysulfate and polysulfonate/K^{+} systems, though the electrostatic interaction between the fixed charge group and divalent ion was stronger than that between the fixed charge group and monovalent ion. For this reason, the *Q* value for CEM07, CEM16, and CEM27 measured in KCl solution is the smallest of all electrolytes. For CEM04, the dielectric constant near the fixed charge groups seem to be so small that the electrostatic interaction between the fixed charge group and the counterion overcomes the effect of hydration on the solute−solute interaction between them because of the low water content. The agreement cited above suggests that ion pairs between the fixed charge group and counterion in the membrane cause the effective charge density estimated by the ionic transport procedure to be less than the fixed charge density, especially for low water content.

Conclusions

In the present study, we prepared charged membranes with low water content and examined their charge effectiveness (*Q*) based on membrane potential measurements in various electrolyte solutions.

(i) The experimental results were analyzed on the basis of the TMS approach considering the inhomogeneous distribution of the fixed charge group in the membrane, because we confirmed the inhomogeneities of fixed charge group distribution from the EDX analysis. The calculated results agreed well with the experimental results. The results show that the charge effectiveness (*Q*) will depend on the membrane water content, the ionic radii of the counterions, and the valence of the counterion.

(ii) Next, to explain these dependences, we attempted to introduce the concept of ion pair between the fixed charge group and counterion inside the membrane. The theoretical prediction considering ion-pair formation qualitatively agreed with the experimental tendencies. This indicates that effect of the ion pairs on the charge effectiveness (*Q*) is substantial in low-water-content charged membranes.

Further studies are required to quantitatively estimate the effect of the ion pair on the ion transport behavior across low-water-content charged membranes.

Acknowledgment. The authors express their appreciation to Mr. Kinoshita, Asahi Kasei Corporation, for providing PE porous membranes.

References and Notes

(1) Saito, K.; Tanioka, A.; Miyasaka, K. *Polymer* **1994**, *35*, 5098.
(2) Kawaguchi, M.; Murata, T.; Tanioka, A. *J. Chem. Soc., Faraday Trans.* **1997**, *93*, 1351.
(3) Matsumoto, H.; Tanioka, A.; Murata, T.; Higa, M.; Horiuchi, K. *J. Phys. Chem. B* **1998**, *102*, 5011.
(4) Glueckauf, E.; Watts, R. E. *Proc. R. Soc. London, A* **1962**, *268*, 339.
(5) Glueckauf, E. *Proc. R. Soc. London, A* **1962**, *268*, 350.
(6) Reiss, H.; Bassignana, I. C. *J. Membr. Sci.* **1982**, *11*, 219.
(7) Selvey, C.; Reiss, H. *J. Membr. Sci.* **1985**, *23*, 11.
(8) Petropoulos, J. H.; Tsimboukis, D. G.; Kouzeli, K. *J. Membr. Sci.* **1983**, *16*, 379.
(9) Petropoulos, J. H. *J. Membr. Sci.* **1990**, *52*, 305.
(10) Larter, R. *J. Membr. Sci.* **1986**, *28*, 165.
(11) Mafé, S.; Manzanares, J. A.; Hernandez, M. J.; Pellicer, J. *J. Colloid Interface Sci.* **1991**, *145*, 433.
(12) Sokirko, A. V.; Manzanares, J. A.; Pellicer, J. *J. Colloid Interface Sci.* **1994**, *168*, 32.
(13) Mafé, S.; Ramírez, P.; Tanioka, A.; Pellicer, J. *J. Phys. Chem. B* **1997**, *101*, 1851.
(14) Chou, T.-J.; Tanioka, A. *J. Membr. Sci.* **1998**, *144*, 275.
(15) Chou, T.-J.; Tanioka, A. *J. Phys. Chem. B* **1998**, *102*, 129.
(16) Chou, T.-J.; Tanioka, A. *J. Phys. Chem. B* **1998**, *102*, 7198.
(17) Teorell, T. *Proc. Soc. Exptl. Biol.* **1935**, *33*, 282.
(18) Teorell, T. *Prog. Biophys. Chem. A* **1953**, *3*, 305.
(19) Meyer, K. H.; Sievers, J. F. *Helv. Chim. Acta* **1936**, *19*, 649, 665, 987.
(20) Donnan, F. G. *Z. Elektrochem.* **1911**, *17*, 572.
(21) Donnan, F. G. *Z. Phys. Chem. A* **1934**, *168*, 369.
(22) Buck, R. P. *J. Membr. Sci.* **1984**, *17*, 1.
(23) Henderson, P. *Z. Physik. Chem.* **1907**, *59*, 118.
(24) Goldman, G. E. *J. Gen. Physiol.* **1943**, *26*, 37.
(25) Mizutani, Y. *J. Membr. Sci.* **1990**, *49*, 121.
(26) Mizutani, Y.; Kusumoto, K.; Nishimura, M.; Nishimura, T.; Asada, E. *J. Appl. Polym. Sci.* **1990**, *39*, 1087.
(27) Mika, A. M.; Childs, R. F.; Dickson, J. M.; McCarry, B. E.; Gagnon, D. R. *J. Membr. Sci.* **1995**, *108*, 37.
(28) Stachera, D. M.; Childs, R. F.; Mika, A. M.; Dicson, J. M. *J. Membr. Sci.* **1998**, *148*, 119.
(29) Choi, Y.-J.; Kang, M.-S.; Moon, S.-H. *Desalination* **2002**, *146*, 287.
(30) Fuoss, R. M. *J. Am. Chem. Soc.* **1958**, *80*, 5059.
(31) Petrucci, S. *Ionic Interactions from dilute solutions to fused salts*, Vol. 1; Academic Press: New York, 1971.
(32) Nightingale, E. R. *J. Phys. Chem.* **1958**, *63*, 1381.
(33) Booth, F. *J. Chem. Phys.* **1951**, *19*, 391.
(34) Verbrugge, M. W.; Hill, R. F. *J. Phys. Chem.* **1988**, *92*, 6778.
(35) Guzmán-Garcia, A. G.; Pintauro, P. N.; Verbrugge, M. W.; Hill, R. F. *AIChE J.* **1990**, *36*, 1061.
(36) Desnoyers, J. E.; Arel, M.; Perron, G.; Jolicoeur, C. *J. Phys. Chem.* **1969**, *73*, 3346.
(37) Salamone, J. C. *Polymeric Materials Encyclopedia*, *Vol. 8*; CRC Press: Boca Raton, FL, 1996.